ELSEVIER

Journal of Photochemistry and Photobiology A: Chemistry 136 (2000) 195–202

Journal of Photochemistry and Photobiology A:Chemistry

www.elsevier.nl/locate/jphotochem

Photolysis of diaryliodonium salts (UV/Vis, EPR and GC/MS investigations)

Viera Jančovičová [a,*], Vlasta Brezová [b], Miroslav Ciganek [c], Zuzana Cibulková [a]

[a] *Department of Printing Arts Technology and Applied Photochemistry, Faculty of Chemical Technology, Slovak Technical University, Radlinského 9, SK-812 37 Bratislava, Slovak Republic*

[b] *Department of Physical Chemistry, Faculty of Chemical Technology, Slovak Technical University, Radlinského 9, SK-812 37 Bratislava, Slovak Republic*

[c] *Institute of Environmental Chemistry, Faculty of Chemistry, Technical University Brno, Purkyňova 118, CZ-612 00, Czech Republic*

Accepted 19 July 2000

Abstract

The photodecomposition of commercial lipophilic diaryliodonium hexafluoroantimonate SarCat® SR-1012 was investigated in acetonitrile (ACN) and ACN/H_2O mixed solvents by means of UV/Vis spectroscopy, an EPR in situ spin trapping technique and GC/MS analysis. The application of the spin traps nitrosodurene (ND) and 5,5-dimethyl-1-pyrroline N-oxide gave evidence for the production of radical intermediates corresponding to the breaking of the carbon–iodine bond, in addition to carbon–oxygen bonds in SR-1012 aryl substitution. The photolytic products analyzed in aprotic acetonitrile were iodobenzene, acetanilide, biphenyl and $C_{12}H_{25}CH(OH)CH_3$, while in ACN/H_2O (1:1, vol.) solution iodobenzene, biphenyl, $C_{12}H_{25}CH(OH)CH_2OC_6H_4OH$ and hydroxylated biphenyls were identified. The influence of oxygen on the product distribution in both solvent systems was inconsequential. The proton concentrations photogenerated in the irradiated SR-1012 ACN/H_2O solutions were quantified spectrophotometrically using bromophenol blue indicator.

Keywords: Iodonium salts; Photolysis; UV/Vis spectroscopy; EPR; Spin trapping; GC/MS analysis

1. Introduction

The diaryliodonium salts with the non-nucleophilic counter ions represent a significant group of cationic photoinitiators, as they have been successfully utilized in the cationic polymerization of epoxides, vinyl ethers and other cationically cured resin systems [1–10]. The photopolymerized materials have properties such that they have found applications in metal, paper and plastic coatings, inks and adhesive products [1–6]. The significant advantage of diaryliodonium salts is their thermal stability in the dark, which facilitates their manipulation as photoinitiators. However, they do not absorb radiation in the visible region because the absorption maxima of variously substituted diaryliodonium salts are between 225 and 275 nm [6,11,12]. Consequently the application of UV radiation is necessary to start the photogeneration of aryliodonium cation-radicals, which initiate the cationic polymerization [5]. The mechanism of the irreversible photodecomposition of diaryliodonium salts is complex, and diverse reaction pathways were described in the literature for the diaryliodonium excited singlet and triplet states [1,2,11–17].

The investigation of the diaryliodonium salts photolysis mechanism is predominantly based on the products analysis, the measurements of protonic acid concentration and on the quantitative determination of iodonium salt consumption which were complicated by the fact that the final products generated in the different reaction pathways were identical [11–13]. Time-resolved laser-spectroscopy experiments were performed in order to establish the transient intermediate formation by direct and sensitized photolysis of variously substituted diaryliodonium salts, and consequently evidence about the photogeneration of aryliodonium cation-radicals upon excitation was obtained [6,17,18]. Sensitized photolysis of lipophilic iodonium salts in various solvents in the presence of both singlet and triplet sensitizers was investigated by the CIDNP technique [19] and fluorescence measurements [16]. The results confirmed that the primary step was an electron transfer from the excited sensitizer to the iodonium cation [15,16,19–21].

Only a few EPR investigations of radicals intermediates produced by photodecomposition of aryliodonium salts were found in the literature [22,23]. The present contribution is

* Corresponding author.
E-mail address: vjancov@chtf.stuba.sk (V. Jančovičová).

1010-6030/00/$ – see front matter
PII: S1010-6030(00)00339-7

focused on the identification of radicals formed by irradiation applying a spin trapping technique. The production of protons upon irradiation of lipophilic iodonium salt was monitored in acetonitrile/water solvents using bromophenol blue indicator.

2. Experimental

2.1. Materials

Lipophilic diaryliodonium salt $\{C_6H_5I^+C_6H_4OCH_2CH(OH)C_{12}H_{25}\}\{(SbF_6)^-\}$ (SarCat® SR-1012) was obtained from Sartomer (USA), *bis*(4-methylphenyl)iodonium chloride (4-MePIC) was synthesized according to the procedure published in Refs. [24,25]. Acetonitrile (ACN, Fluka, Germany) was used without further purification. Bromophenol blue and *p*-toluenesulfonic acid were purchased from Lachema (Czech Republic). The spin traps nitrosodurene (ND) and 5,5-dimethyl-1-pyrroline N-oxide (DMPO) from Aldrich (UK) were applied. DMPO was freshly redistilled before use and stored under argon in a freezer. Deionized water was used in the preparation of solutions.

2.2. Methods and apparatus

The solutions were irradiated in a quartz cell (1-cm path length) using apparatus with a focused light beam from a 400 W medium pressure mercury lamp (RWK, Holešovice, Czech Republic). A Pyrex filter was used to cut-off the radiation below 300 nm. The samples were purged with nitrogen 15 min before irradiation, or the solutions were stored under air. All photochemical experiments were performed at a temperature of 295 K.

The source light flux (2.9×10^{-8} mol s^{-1}, corresponding to the light intensity of 5 mW cm^{-2}) was determined by a standard procedure using ferrioxalate actinometry [26]. The monochromatic light beams with $\lambda = 313$ nm, as well as with $\lambda = 325$ nm, were selected using optical filters (Schott Glaswerke, Germany) in the actinometric experiments. The UV/Vis spectra were recorded using a UV/Vis spectrometer PU 8800 (Philips, UK).

The EPR spectra were measured at a temperature of 290 K using a Bruker 200D spectrometer (Germany) interfaced to an Aspect 2000 computer (Germany). The standard spectrometer settings were as follows: center field, 349 mT; sweep width, 10 mT; scan time, 50 or 100 s; microwave frequency, 9.72 GHz; microwave power, 10 mW; modulation amplitude, 0.005–0.05 mT; spectrometer gain, 10×10^4–5×10^5. The freshly prepared solutions containing spin traps ($c_{DMPO} = 0.01$ M; saturation concentrations of ND under the given experimental conditions) were carefully purged with argon, then placed in a quartz cell optimized for the Bruker TM cavity. The samples were irradiated directly in the cavity with light from a 250 W medium pressure mercury lamp (Applied Photophysics, England), and the EPR spectra were monitored in situ. A Pyrex filter was used to cut-off the radiation below 300 nm. The *g*-value was determined with an uncertainty of ±0.0001 using a marker containing 1,1-diphenyl-2-picrylhydrazyl (DPPH) built into the EPR spectrometer. The simulations of the EPR spectra were obtained using the program EPR *SimFonia* (Bruker, Germany). The complex experimental EPR spectra were fitted as the linear combinations of the individual simulations according to a least-squares procedure using the Scientist program (MicroMath).

The formation of H^+ ions in the samples containing water was monitored spectrophotometrically using bromophenol blue, by following the absorbance decrease at $\lambda = 595$ nm caused by pH reduction. The concentration of H^+ ions generated in the irradiated solutions of SR-1012 was calculated by means of bromophenol blue calibration curves measured in the presence of accurate concentrations of *p*-toluenesulfonic acid.

GC/MS analysis was performed using GC/MS apparatus (GC 6200, MS Trio 1000 from Fisons Instruments), with capillary column DB-MSITD (30 m; ID 0.25 mm; stationary phase film 0.25 μm). The samples irradiated in mixed solvents ACN/H_2O (volume 1 μl) were extracted in 1 ml of isooctane, and 1 μl of the prepared extracts was used in the analysis.

3. Results and discussion

3.1. Photolysis of SR-1012

Fig. 1 illustrates the characteristic sets of UV/Vis spectra measured during the irradiation of the lipophilic iodonium salt SR-1012 in the acetonitrile solutions under nitrogen or air. In both experimental systems, upon illumination the absorption maximum of SR-1012 at $\lambda = 250$ nm decreased, and a new absorption peak with maximum at $\lambda = 230$ nm was formed, the intensity of which increased considerably with prolonged irradiation time. Additional GC/MS analysis confirmed that this absorption is characteristic of iodobenzene which represents, according to the mechanisms proposed for the photolysis of iodonium salts, the main degradation product [11–17]. However, the UV/Vis spectra could not be used for the quantification of photoproduced iodobenzene, as other photolytic products also absorbed radiation in this region. The UV/Vis spectra shown in Fig. 1a and b demonstrate that oxygen has a negligible influence on the photolysis of SR-1012. An analogous effect was observed previously in the photolysis of diaryliodonium salts, where the measured quantum yields of iodonium salts associated with the disappearance of the salt and of the protonic acid formation were not influenced by the presence of oxygen. This observation was rationalized in terms of the very short lifetimes of the iodonium salt excited states ($\tau < 10^{-8}$ s) [11].

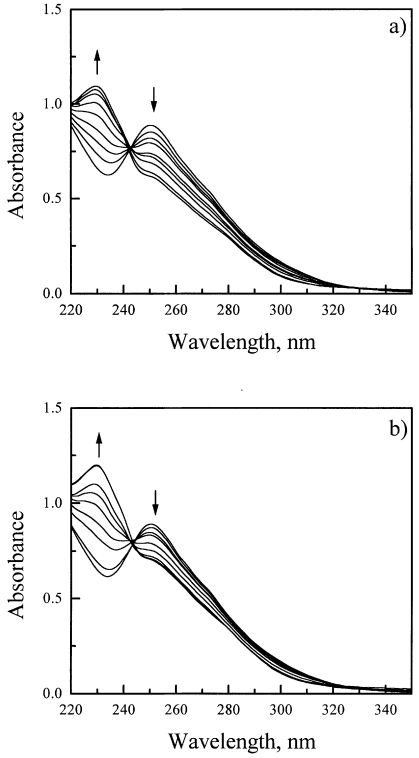

Fig. 1. Changes in the UV/Vis spectra monitored during the irradiation of SR-1012 in acetonitrile solutions ($c_0 = 70\,\mu\text{mol dm}^{-3}$) under: (a) nitrogen; (b) air. Exposure: 0, 1, 2, 3, 5, 7, 10, 20 and 30 min. Cell length: 1 cm.

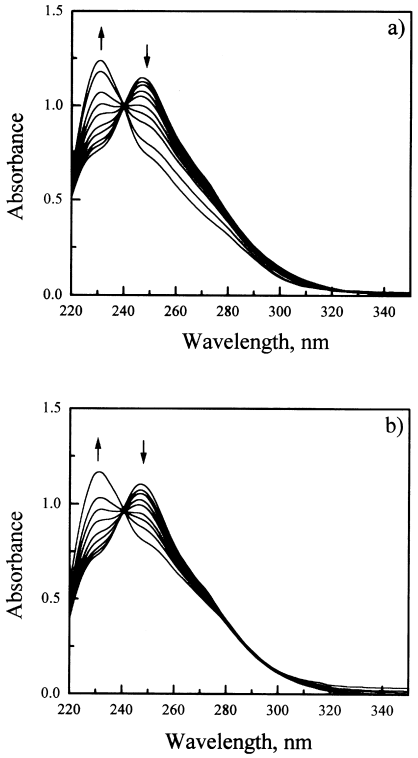

Fig. 2. Changes in the UV/Vis spectra measured during the irradiation of SR-1012 in ACN/H_2O (1:1, vol.) solutions ($c_0 = 70\,\mu\text{mol dm}^{-3}$) under: (a) nitrogen; (b) air. Exposure: 0, 0.5, 1, 2, 3, 5, 7, 10 and 20 min. Cell length: 1 cm.

The set of UV/Vis spectra measured during photolysis of SR-1012 in the solvent mixture ACN/H_2O (1:1, vol.) under nitrogen and air atmosphere is depicted in Fig. 2. The changes in UV/Vis spectra unambiguously indicated that the photolysis of iodonium salt is influenced by water present in the experimental systems. This proposition was supported by EPR spin trapping experiments and GC/MS analysis as will be shown below. On the other hand, once again the unimportant consequence of the presence of oxygen was observed under the given experimental conditions.

3.2. Spectrophotometric determination of photoproduced H^+ ion concentrations

The formation of H^+ ions during the photolysis of SR-1012 in ACN/H_2O (1:1, vol.) solutions was investigated by the addition of bromophenol blue into the experimental systems. However, the application of bromophenol blue was not suitable for water-free acetonitrile solutions. The satisfactory photostability of bromophenol blue was confirmed in the photochemical blank experiments under given experimental conditions.

The changes in UV/Vis spectra of bromophenol blue caused by the decrease in pH during photolysis of SR-1012 in ACN/H_2O (1:1, vol.) solutions is shown in Fig. 3. The results confirm that the formation of H^+ ions could be easily monitored by means of bromophenol blue absorbance reduction at $\lambda = 595$ nm, as illustrated in the inset in Fig. 3. The measured spectral data were exploited for the determination of photoproduced proton concentrations in the irradiated SR-1012 solutions applying the calibration curves.

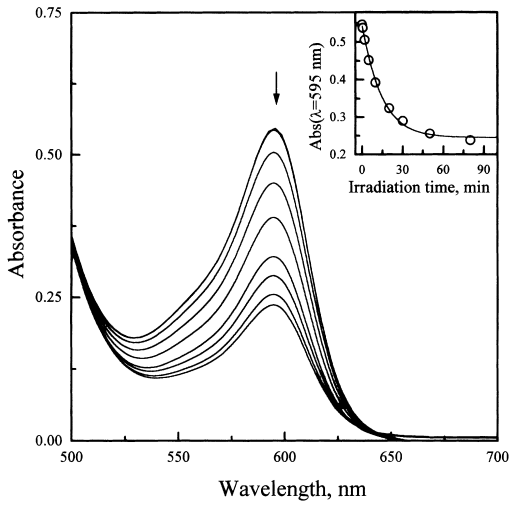

Fig. 3. Changes in the UV/Vis spectra of bromophenol blue ($c_{BB} = 75\,\mu\text{mol dm}^{-3}$) upon irradiation of SR-1012 ($c_0 = 70\,\mu\text{mol dm}^{-3}$) in ACN/$H_2O$ (1:1, vol.) solutions under nitrogen. Exposure: 0, 0.5, 2, 5, 10, 20, 30, 50 and 80 min. Cell length: 1 cm. Inset: the dependence of bromophenol blue absorbance at $\lambda = 595$ nm on the irradiation time.

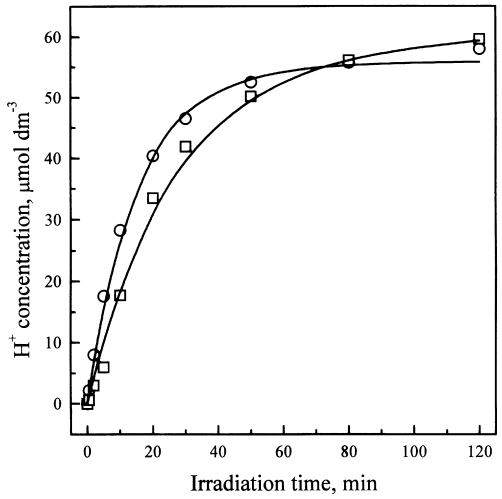

Fig. 4. The dependence of H^+ ion concentration on the irradiation time consequent to the irradiation of SR-1012 ($c_0 = 70\,\mu mol\,dm^{-3}$) in ACN/$H_2O$ (1:1, vol.) solutions under nitrogen (○) or air (□).

Fig. 4 illustrates the dependence of H^+ ion concentration, c_{H^+}, on the irradiation time measured in SR-1012 ACN/H_2O (1:1, vol.) solutions under nitrogen or air. The experimental data depicted in Fig. 4 were fitted by the non-linear least-squares minimization procedure to a saturation exponential curve (Eq. (1)), and the initial rate of H^+ ion formation, r_0, was evaluated (Eq. (2))

$$c_{H^+} = c_{H^+\infty}(1 - \exp(-kt_{exp})) \quad (1)$$

$$r_0 = \left(\frac{dc_{H^+}}{dt_{exp}}\right)_{t_{exp}=0} = c_{H^+\infty}k \quad (2)$$

where $c_{H^+\infty}$ is the limiting H^+ ion concentration, k the formal first-order rate constant and t_{exp} the irradiation time.

The calculated values of k, $c_{H^+\infty}$ and r_0 obtained from the experimental data shown in Fig. 4 are summarized in Table 1. The lower value of the initial rate of H^+ ion formation in the oxygenated solutions (Table 1), indicates the role of oxygen in the deactivation of the photogenerated reactive intermediates creating H^+ ions. However, the influence of oxygen on the limiting proton concentrations is insignificant under the given experimental conditions. Despite the low absorption of SR-1012 over 300 nm (Figs. 1 and 2), and application of a Pyrex filter to cut off the radiation below 300 nm in our experimental arrangement, the limiting proton concentrations obtained in ACN/H_2O (1:1, vol.) solutions under nitrogen or air were in accord with the initial SR-1012 concentration used in the experiments ($c_0 = 70\,\mu mol\,dm^{-3}$).

Table 1
The value of the formal rate constant, limiting H^+ ion concentrations and initial rate of proton formation evaluated by a non-linear least-squares fit of the experimental data shown in Fig. 4 to a saturation curve (Eq. (1))

Atmosphere	k (min^{-1})	$c_{H^+\infty}$ ($\mu mol\,dm^{-3}$)	r_0 ($\mu mol\,dm^{-3}\,min^{-1}$)
Nitrogen	0.067	55.8	3.7
Air	0.037	60.0	2.2

3.3. EPR spin trapping experiments

In accordance with the proposed mechanisms, the photolysis of iodonium salts can be initiated by homolytic, as well as heterolytic, cleavage of carbon–iodine bond forming the reactive radical and cation-radical species [1,2,11–17]. In the present work, we have attempted to apply in situ EPR spectroscopy for the characterization of intermediates produced upon irradiation of the SR-1012 iodonium salt. Unfortunately, the stationary-state concentrations of the photoproduced species were too low for a direct EPR identification, and no EPR spectra were observed. Consequently, we exploited a spin trapping technique using ND and DMPO spin traps. These compounds were chosen because of their relatively high photostability in the photochemical spin trapping experiments [27–29].

Upon continuous irradiation of lipophilic iodonium salt SR-1012 in acetonitrile solutions in the presence of ND spin trap, two radical adducts were monitored, i.e., $^{\bullet}ND–C_6H_5$ and $^{\bullet}ND–CH_2CN$ (Fig. 5). Their spin Hamiltonian parameters are summarized in Table 2. The stability of $^{\bullet}ND–CH_2CN$ adduct after radiation cessation is lower under given experimental conditions, accordingly their relative EPR intensity rapidly decreased after the irradiation source was removed, and in the observed EPR spectra the signal of $^{\bullet}ND–C_6H_5$ adduct predominated (Fig. 5). The

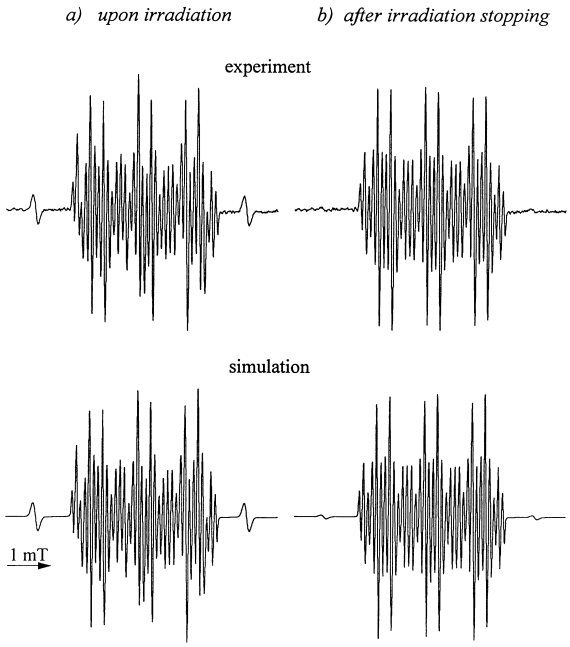

Fig. 5. Experimental and simulated EPR spectra of $^{\bullet}$ND-adducts observed (a) upon continuous irradiation and (b) after the source of irradiation was removed in SR-1012 acetonitrile solutions ($c_0 = 0.7\,mmol\,dm^{-3}$; the solutions were saturated with ND).

formation of $^{\bullet}C_6H_5$ and $^{\bullet}CH_2CN$ radicals upon irradiation of SR-1012 is fully compatible with the mechanism published by Timpe and Schikowsky [11] for iodonium salts photolysis in acetonitrile solutions. In previous experiments, the generation of $^{\bullet}ND–C_6H_5$ adduct was confirmed by the spin trapping technique using nitrosodurene during the photodecomposition of diphenyliodonium salt [22].

However, the experiments using DMPO spin trap in the irradiation of SR-1012 in acetonitrile solutions revealed further information about the reaction mechanism. Analysis of the complex EPR spectra measured upon continuous exposure established that, in addition to low concentrations of $^{\bullet}$DMPO–C adduct, corresponding to $^{\bullet}C_6H_5$ addition, we monitored significant signals corresponding to two $^{\bullet}$DMPO-adducts with different alkoxyl radicals, i.e., $^{\bullet}$DMPO–OR_{arom} and $^{\bullet}$DMPO–OR_{alif} (Fig. 6 and Table 2). Consequently, in the aprotic acetonitrile solvent we observed not only radical intermediates produced by cleavage of carbon–iodine bond, but also by splitting of carbon–oxygen bonds in SR-1012 substitution. This hypothesis was supported by the GC/MS analysis of SR-1012 photolytic products, when $C_{12}H_{25}CH(OH)CH_3$ was detected selectively in acetonitrile. In addition, a triplet, characterized by the nitrogen splitting constant $a_N = 1.412$ mT (Table 2), was also observed in the experimental EPR spectra (Fig. 6). This is most likely originated from DMPO degradation during irradiation.

The spin trapping experiments in mixed solvents with various ACN/H_2O ratios using nitrosodurene, again established the formation of $^{\bullet}C_6H_5$ and $^{\bullet}CH_2CN$ radicals during irradiation of the SR-1012 iodonium salt. However, addition of water caused changes in the relative EPR intensity of both adducts monitored during continuous irradiation. Thus, the nine-line EPR spectrum of $^{\bullet}ND–CH_2CN$ radical predominated in ACN/H_2O (1:1, vol.) solvent (Fig. 7 and Table 3). This observation can probably be attributed to the lowered solubility of the ND spin trap in ACN/H_2O solvents, which is reflected in the lower quality of the EPR spectra obtained with the increasing amounts of water in mixed solvents (Fig. 7).

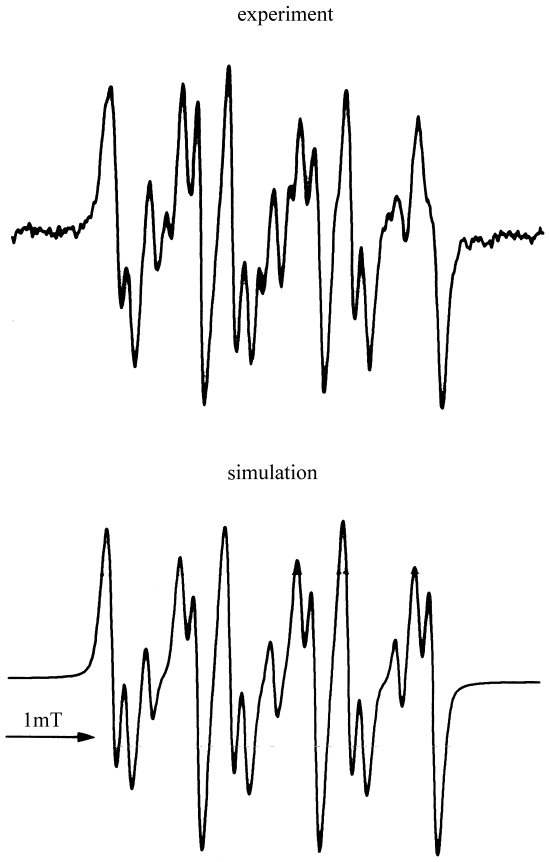

Fig. 6. Experimental and simulated EPR spectra of $^{\bullet}$DMPO-adducts observed upon continuous irradiation of SR-1012 in acetonitrile ($c_0 = 0.7$ mmol dm^{-3}; $c_{DMPO} = 0.01$ mol dm^{-3}).

The EPR spectra observed using DMPO upon photolysis of SR-1012 in ACN/H_2O (9:1, vol.) solvents were substantially changed (Fig. 8), compared with those measured in acetonitrile solvent (Fig. 6). Presumably, the presence of water initiated the formation of new types of radicals in the experimental systems. Previously, Timpe and Schikowsky [11] proposed that in the ACN/H_2O environment the formation

Table 2
Parameters used in the simulations of the experimental EPR spectra measured upon continuous irradiation of acetonitrile SR-1012 solutions in the presence of the spin traps ND or DMPO (Figs. 5 and 6)

Spin trap	Splitting constant (mT)		*g*-factor	Adduct	Relative area (%)	References
	a_N	a_H				
ND	1.355	0.975 (2H)	2.0060	$^{\bullet}CH_2CN$	38	[30–33]
ND	1.055	0.295 (2H^{o}) 0.095 (2H^{m}) 0.273 (H^{p})	2.0057	$^{\bullet}C_6H_5$	62	[22,30–33]
DMPO	1.440	2.134	2.0058	$^{\bullet}C_6H_5$	2	[31,33,34]
DMPO	1.333	1.069 0.136 (H$^{\gamma}$)	2.0060	$^{\bullet}OR_{arom}$	37	[33,35]
DMPO	1.330	0.795 0.172 (H$^{\gamma}$)	2.0059	$^{\bullet}OR_{alif}$	60	[33,36]
DMPO	1.412	–	2.0058	DMPO degradation	1	[33,37]

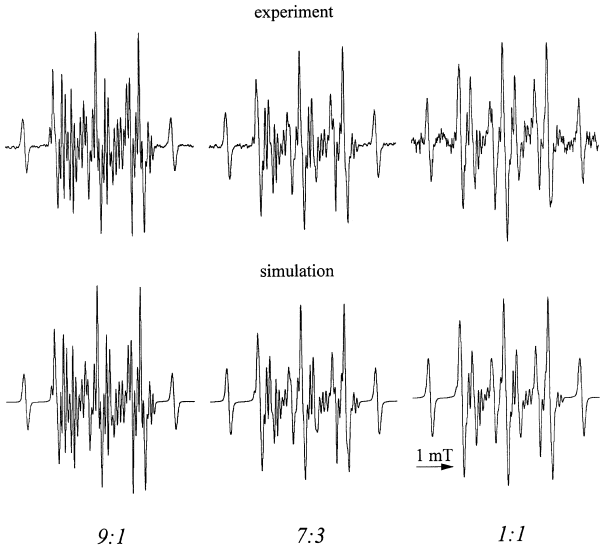

Fig. 7. Experimental and simulated EPR spectra of •ND-adducts measured upon continuous irradiation of SR-1012 in various ACN/H_2O (v/v, vol.) solutions ($c_0 = 0.7\,\text{mmol dm}^{-3}$; solutions were saturated with ND).

of •Aryl(IOH) radicals occurs by the reaction of photoproduced aryliodonium cation-radical with water (Eq. (3)). Radicals •Aryl(IOH) can terminate by the different pathways, and the generation of hydroxyl radicals (Eq. (4)) represents one possibility. In addition, in an aquatic environment, the hydroxyl radicals can also be generated by the termination of different photoproduced aryl radicals with water

$$\text{Aryl}^{\bullet+} + \text{H}_2\text{O} \rightarrow {}^{\bullet}\text{Aryl(IOH)} + \text{H}^+ \quad (3)$$

$$^{\bullet}\text{Aryl(IOH)} \rightarrow \text{ArI} + {}^{\bullet}\text{OH} \quad (4)$$

The experimental EPR signal shown in Fig. 8a, was simulated as a linear combination of three individual EPR spectra corresponding to a six-line •DMPO–C_6H_5, four-line •DMPO–R, and a triplet spectrum representing DMPO photodegradation product (Table 4). However, an essential problem was the assignment of •DMPO–R adduct. Consequently, in an attempt to solve this problem, we performed identical EPR experiments using the spin trap DMPO irradiating the symmetrical *bis*(4-methylphenyl)iodonium chloride in ACN/H_2O (1:1, vol.) solvent. Surprisingly, using 4-MePIC we obtained an identical EPR spectrum to that obtained in the photolysis of the SR-1012 salt (Fig. 9, Table 4). Accordingly, and with reference to the mechanism

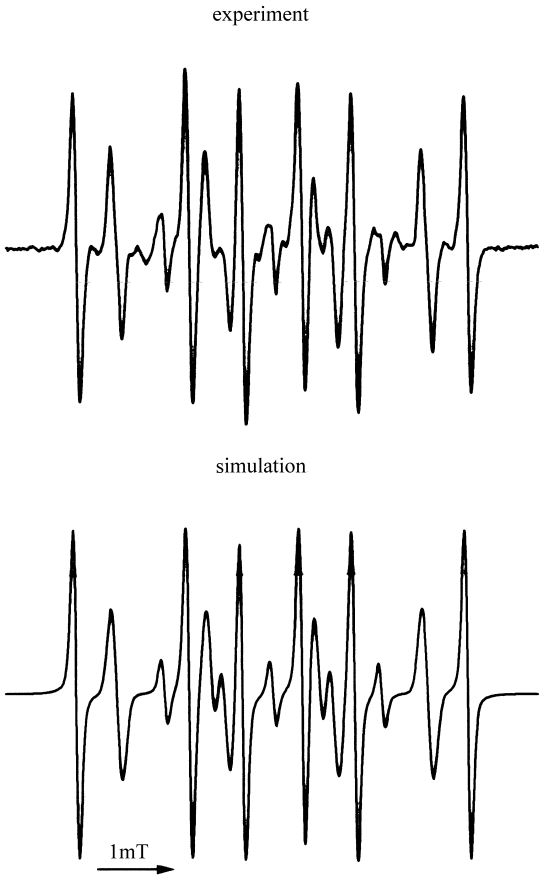

Fig. 8. Experimental and simulated EPR spectra of •DMPO-adducts measured upon continuous irradiation of SR-1012 in ACN/H_2O (9:1, vol.) solution ($c_0 = 0.7\,\text{mmol dm}^{-3}$; $c_{\text{DMPO}} = 0.01\,\text{mol dm}^{-3}$).

Table 3
Parameters used in the simulations of the experimental EPR spectra measured upon continuous irradiation of SR-1012 solutions in various ACN/H_2O solvents in the presence of the spin trap ND (Fig. 7)

ACN/H_2O solvent system (vol.)	•ND–C_6H_5			•ND–CH_2CN		
	Splitting constant (mT)		Relative area (%)	Splitting constant (mT)		Relative area (%)
	a_N	a_H		a_N	a_H	
9:1	1.076	0.292 (2H^o) 0.097 (2H^m) 0.290 (H^p)	45	1.367	0.992 (2H)	55
7:3	1.099	0.298 (2H^o) 0.098 (2H^m) 0.298 (H^p)	22	1.380	1.006 (2H)	78
1:1	1.123	0.304 (2H^o) 0.100 (2H^m) 0.303 (H^p)	14	1.410	1.020 (2H)	86

Table 4
Parameters used in the simulations of the experimental EPR spectra measured upon continuous irradiation of ACN/H_2O (1:1, vol.) SR-1012 and 4-MePIC solutions in the presence of the spin trap DMPO (Fig. 9)

Iodonium salt	Splitting constant (mT)		*g*-factor	Adduct	Relative area (%)	References
	a_N	a_H				
SR-1012	1.535	2.285	2.0058	$^{\bullet}C_6H_5$	48	[33,37]
SR-1012	1.465	1.365	2.0059	$^{\bullet}OH$	49	[34,38]
SR-1012	1.450	–	2.0058	DMPO degradation	3	[37]
4-MePIC	1.485	2.210	2.0058	$^{\bullet}CH_2CN$	1.6	–
4-MePIC	1.538	2.290	2.0058	$^{\bullet}C_6H_4CH_3$	25	[37]
4-MePIC	1.465	1.365		$^{\bullet}OH$	73	[34,38]
4-MePIC	1.450	–	2.0058	DMPO degradation	0.4	[37]

proposed by Timpe and Schikowsky [11], the four-line EPR signal ($^{\bullet}$DMPO–R) measured in ACN/H_2O solvents was attributed to the $^{\bullet}$DMPO–OH adduct.

3.4. GC/MS analysis of SR-1012 photolysis products

GC/MS analysis was applied in an effort to identify the SR-1012 degradation products. Table 5 schematically represents the results of the qualitative analysis of SR-1012 samples irradiated 20 min in acetonitrile, as well as in ACN/H_2O (1:1, vol.) solvents under either a nitrogen or an air atmosphere. The information base obtained can be summarized as follows:

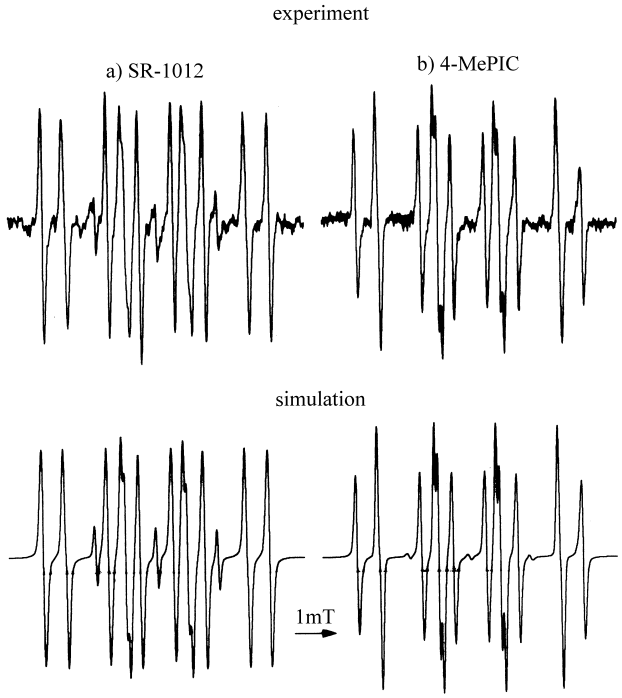

Fig. 9. (a) Experimental and simulated EPR spectra of $^{\bullet}$DMPO-adducts obtained upon continuous irradiation of SR-1012 in ACN/H_2O (1:1, vol.) solutions ($c_0 = 0.7\,\text{mmol dm}^{-3}$; $c_{DMPO} = 0.01\,\text{mol dm}^{-3}$); (b) Experimental and simulated EPR spectra of $^{\bullet}$DMPO-adducts obtained upon continuous irradiation of 4-MePIC in ACN/H_2O (1:1, vol.) solutions ($c_0 = 3\,\text{mmol dm}^{-3}$; $c_{DMPO} = 0.01\,\text{mol dm}^{-3}$).

Table 5
Summary of the results of GC/MS analysis of SR-1012 samples irradiated 20 min in acetonitrile, as well as in ACN/H_2O (1:1, vol.) solvents under either a nitrogen or an air atmosphere

Product	Solvent			
	Acetonitrile under		ACN/H_2O (1:1, vol.) under	
	N_2	Air	N_2	Air
Iodobenzene	Yes	Yes	Yes	Yes
Acetanilide	Yes	Yes	No	No
Biphenyl	Yes	Yes	Yes	Yes
$C_{12}H_{25}CH(OH)CH_3$	Yes	Yes	No	No
$C_{12}H_{25}CH(OH)CH_2OC_6H_4OH$	No	No	Yes	Yes
Hydroxylated biphenyls	No	No	Yes	Yes

- GC/MS analysis identified the products of both homolytic and heterolytic cleavages of the carbon–iodine bond in the SR-1012 molecule. The main degradation product in different solvent systems is iodobenzene.
- The effect of oxygen on the product distribution is inconsequential in acetonitrile, as well as in ACN/H_2O solvents.
- The products of SR-1012 photolysis in acetonitrile and ACN/H_2O mixed solvents are different. (These results were supported by measured differences in UV/Vis spectra upon irradiation, and by radical intermediates identified in in situ spin trapping experiments, respectively.) Acetanilide was formed only in acetonitrile and was probably produced by the Ritter reaction [11,13] of aryl cation with ACN. In addition, the formation of $C_{12}H_{25}$-$CH(OH)CH_3$ validated the cleavage of the carbon–oxygen bond, evidenced also by EPR spin trapping experiments in acetonitrile. Hydroxylated products were formed exclusively in the mixed solvents ACN/H_2O, presumably by the reaction of the corresponding cation-radicals and radicals with water.

4. Conclusions

The radical intermediates ($^{\bullet}C_6H_5$, $^{\bullet}CH_2CN$, $^{\bullet}OR_{arom}$, $^{\bullet}OR_{alif}$, $^{\bullet}OH$) generated upon irradiation ($\lambda > 300$ nm) of lipophilic diaryliodonium hexafluoroantimonate SR-1012

in acetonitrile and acetonitrile/water solvent systems were identified utilizing a spin trapping technique with ND and DMPO spin traps. Thus, $^{\bullet}C_6H_5$ and $^{\bullet}CH_2CN$ were measured under all conditions, but alkoxyl adducts were monitored exclusively in acetonitrile, and $^{\bullet}$DMPO–OH in mixed solvents containing water, respectively. The results of an EPR spin trapping technique, as well as UV/Vis spectroscopy and GC/MS analysis established different reaction pathways in aprotic acetonitrile and in ACN/H_2O mixed solvents. The proton concentrations produced by irradiation of SR-1012 in ACN/H_2O solutions were quantified spectrophotometrically using bromophenol blue indicator.

Acknowledgements

We thank the Slovak Grant Agency for the financial support (Projects VEGA/1/6156/99 and VEGA/1/7313/20), and the Sartomer Company for the gift of diaryliodonium salt SarCat® SR-1012 sample.

References

[1] H.-J. Timpe, in: J.-P. Fouassier, J.F. Rabek (Eds.), Radiation Curing in Polymer Science and Technology, Vol. 2, Photoinitiating Systems, Elsevier, Amsterdam, 1993, p. 529.
[2] J.V. Crivello, in: J.-P. Fouassier, J.F. Rabek (Eds.), Radiation Curing in Polymer Science and Technology, Vol. 2, Photoinitiating Systems, Elsevier, Amsterdam, 1993, p. 435.
[3] J.V. Crivello, D.A. Conlon, J. Polym. Sci. A 21 (1983) 1785.
[4] F. Loshe, H. Zweifel, Adv. Polym. Sci. 78 (1986) 61.
[5] C. Decker, in: H.E.H. Meijer (Ed.), Processing of Polymers, Vol. 18, Materials Science and Technology, R.W. Cahn, P. Haasen, E.J. Kramer (Eds.), VCH Verlaggesellschaft, Weinheim, 1997, p. 615.
[6] J.-P. Fouassier, D. Burr, J.V. Crivello, J.M.S. Pure Appl. Chem. A 31 (1994) 677.
[7] R. Muneer, T.W. Nalli, Macromolecules 31 (1998) 7976.
[8] K.S. Feng, H.M. Zang, D. Martin, T.L. Marino, D.C. Neckers, J. Polym. Sci. A 36 (1998) 1667.
[9] J.V. Crivello, S.S. Liu, J. Polym. Sci. A 37 (1999) 1199.
[10] S. Kaur, J.V. Crivello, N. Pascuzzi, J. Polym. Sci. A 37 (1999) 199.
[11] H.-J. Timpe, V. Schikowsky, J. Prakt. Chem. 331 (1989) 447.
[12] J.-P. Fouassier, Photoinitiation, Photopolymerization, and Photocuring. Fundamentals and Applications, Carl Hanser, Munich, 1995, p. 102.
[13] J.L. Daktar, N.P. Hacker, J. Org. Chem. 55 (1990) 639.
[14] J.A. Kampmeier, T.W. Nalli, J. Org. Chem. 59 (1994) 1381.
[15] A. Kunze, U. Müller, K. Tittes, J.-P. Fouassier, F. Morlet-Savary, J. Photochem. Photobiol. A 110 (1997) 115.
[16] U. Müller, I. Zücker, J. Photochem. Photobiol. A 120 (1999) 93.
[17] R.J. De Voe, M.R. Sahyun, N. Serpone, D.K. Sharma, Can. J. Chem. 65 (1987) 2342.
[18] E. Klemm, E. Riesenberg, A. Graneβ, Z. Chem. 23 (1983) 222.
[19] M. Goez, G. Eckert, U. Müller, J. Phys. Chem. A 103 (1999) 5714.
[20] W.E. Nelson, T.P. Carter, A.B. Scranton, J. Polym. Sci. A 33 (1995) 247.
[21] G. Eckert, M. Goez, B. Maiwald, U. Müller, Ber. Bunsenges. Phys. Chem. 100 (1996) 1191.
[22] M. Fedurco, P. Rapta, P. Kuran, L. Dunsch, Ber. Bunsenges. Phys. Chem. 101 (1997) 1045.
[23] Y.V. Razskazovskii, M.J. Raiti, M.D. Sevilla, J. Phys. Chem. A 103 (1999) 6351.
[24] F.M. Beringer, M. Drexler, E.M. Gindler, C.C. Lumpkin, J. Am. Chem. Soc. 75 (1953) 2705.
[25] F.M. Beringer, H.E. Bachofner, R.A. Falk, M. Laff, J. Am. Chem. Soc. 80 (1958) 4279.
[26] A.M. Braun, M.-T. Maurette, E. Oliveros, Technologie Photochimique, Presses Polytechniques Romandes, Lausanne, 1986, p. 68.
[27] R. Konaka, S. Terabe, T. Mizuta, S. Sakata, Can. J. Chem. 60 (1982) 1532.
[28] K.J. Reszka, C.F. Chignell, Photochem. Photobiol. 60 (1994) 442.
[29] K.J. Reszka, P. Bilski, R.H. Sik, C.F. Chignell, Free Rad. Res. Commun. 19 (1993) S33.
[30] K. Erentová, V. Adamčík, A. Staško, O. Nuyken, A. Lang, M.B. Leitner, Collect. Czech. Chem. Commun. 62 (1997) 855.
[31] A. Staško, P. Rapta, V. Brezová, O. Nuyken, R. Vogel, Tetrahedron 49 (1993) 10917.
[32] D. Rehorek, E.G. Janzen, J. Prakt. Chem. 326 (1984) 935.
[33] A. Staško, K. Erentová, P. Rapta, O. Nuyken, B. Voit, Magn. Reson. Chem. 36 (1998) 13.
[34] P. Barker, A.L.J. Bechwith, W.R. Cherry, R. Huie, J. Chem. Soc. Perkin Trans. 2 (1985) 1147.
[35] A. Staško, K. Szaboová, V. Cholvad, O. Nuyken, J. Dauth, J. Photochem. Photobiol. A 69 (1993) 295.
[36] K.M. Schaish, D.C. Borg, Free Rad. Res. Commun. 9 (1990) 267.
[37] V. Cholvad, K. Szaboová, A. Staško, O. Nuyken, B. Voit, Magn. Reson. Chem. 29 (1991) 402.
[38] T. Ozawa, A. Hanaki, Chem. Pharm. Bull. 26 (1978) 2572.